

Role of shamal and easterly winds on the wave characteristics off Qatar, central Arabian Gulf

V.M. Aboobacker¹, S.V. Samiksha², S. Veerasingam¹, Ebrahim M.A.S. Al-Ansari¹, P. Vethamony^{1*}

¹Environmental Science Center, Qatar University, P.O. Box 2713, Doha, Qatar

²CSIR-National Institute of Oceanography, Dona Paula, Goa - 403 004, India

* Corresponding author, email: pvethamony@qu.edu.qa

Abstract

Waves in the Arabian Gulf (Gulf) are dominated by shamal winds during winter and early summer. Although wave characteristics in the Gulf are broadly studied, features associated with various wind systems are not explicitly covered, especially in the Exclusive Economic Zone (EEZ) of Qatar. In this study, we analyzed the wave parameters measured off Fuwairit, north coast of Qatar during 29 Oct – 26 Nov 2019 to identify the features associated with different wind systems. The analyses have been further extended to the Gulf using the reanalysis waves obtained from the COPERNICUS Marine Environment Monitoring Services (CMEMS) to describe the monthly, seasonal and annual characteristics. Results indicate that Nashi winds influence the east and northeast coasts of Qatar with higher waves than those generated by shamal winds. We find exceptional easterly (Nashi) waves during March 2019 contributing to the highest monthly mean H_s , which is a deviation from the known long-term wave climate of the Gulf.

Keywords: Waves off Qatar; Arabian/Persian Gulf; Nashi winds; Shamal winds; Shamal waves; CMEMS reanalysis waves.

1. Introduction

Surface waves, driven by the winds, are one of the major controlling factors for the coastal dynamics. For instance, longshore current and sediment transport are highly influenced by nearshore wave transformation. The activities such as design of coastal and offshore structures, exploitation of conventional resources, loading and unloading, navigation and recreational activities are relied on accurate information of surface waves. Wave statistics derived from point measurements are generally used to describe the inherent features of waves in that region. Temporal and spatial analyses is usually carried out using wave model results or satellite observations. Though most of the studies in the Indian Ocean are for open ocean or coastal regions (Sirisha, et al., 2017; Samiksha et al., 2012), very few studies are carried out for the semi-enclosed/marginal seas (Langodan et al., 2014). Wave characteristics on marginal seas gained more attention in recent years, particularly because of their links with dominant local/regional features and global climate indices (Shanas et al., 2017).

The Arabian/Persian Gulf (hereafter referred to as “Gulf”) is a semi-enclosed sea connecting the Arabian Sea through the Strait of Hormuz and the Sea of Oman (Figure 1). The Strait of Hormuz is narrow with a minimum width of 39 km (Van Dyke, 2008). The central Gulf is characterised by the Exclusive Economic Zone (EEZ) of Qatar in the south and the EEZ of Iran in the north. The EEZ of Qatar is relatively wider off the east and north of Qatar, but very narrow off west of Qatar. North and east coasts of Qatar are exposed to the complex dynamic interactions of the Gulf with the Arabian Sea (Pous et al., 2015). The topographic features of the Gulf are complex bathymetry, numerous small and big islands, coral reefs, seagrass meadows, mangrove forests and mud/sand flats (Khan et al., 2002). The climatic features of the Gulf are extreme hot summer, moderate cold winter, high evaporation, weak precipitation, shamal winds and dust storms.

The winds over the Gulf predominantly varies between northwest (NW) to north (N) throughout the seasons, while east (E) to southeast (SE) winds prevail occasionally (Thoppil and Hogan, 2010). The strongest winds in the Gulf are associated with shamal events (Notaro et al., 2015). Shamal events, the unique weather phenomena over the Arabian Peninsula, occur throughout the year, but predominantly during winter and early summer (Perrone, 1979). The summer shamal is caused by a steep pressure gradient formed between the northwest India (low pressure) and the eastern Mediterranean Sea (high pressure), while the winter shamal is associated with mid-latitude disturbances moving from west to east. The shamal periodicities are generally of two kinds: shorter events of 24–36 h and longer events of 3–5 days, based on their intensity and spatial distribution (Aboobacker et al., 2011). The higher wind speeds during shamal events are observed in the northern

and central Arabian Gulf (Liao and Kaihatu, 2016a). The higher mean wind speed (of the order of 5.9 m/s) during winter is observed in the central Gulf, whereas higher mean wind speed (of the order of 4.9 m/s) during summer is in the northern Gulf. The annual mean wind speeds along the Qatar coast varies between 3.0 and 5.0 m/s, whereas the 95th percentile wind speed is between 8.0 and 12.0 m/s (Patlakhas et al., 2019). Though winds are predominantly in the NW/NNW direction, sea-land breezes from various directional sectors are also present when the regional wind systems weaken (Sandeepan et al., 2018).

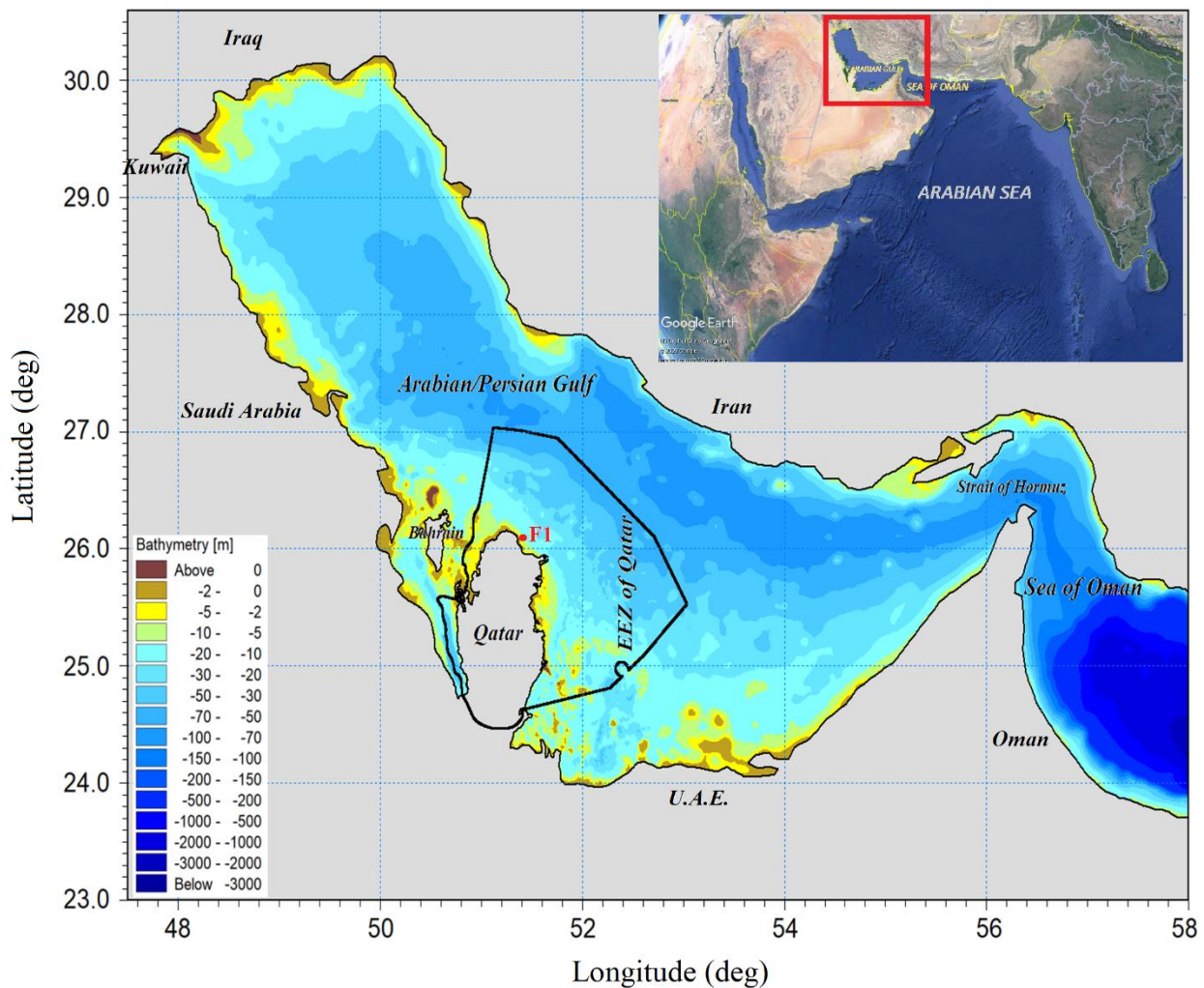


Figure 1. Study area: Bathymetry of the Gulf and the Exclusive Economic Zone (EEZ) of Qatar. Wave measurement location off Fuwairit (F1) is marked in red. The thick black line indicates the boundary of the EEZ.

The Gulf being a semi-enclosed sea, waves in the Gulf follows the prevailing wind patterns with relatively high impact on shamal events (Kamranazad, 2013). The wider deflection in the orientation of the coastline adjacent to the Strait of Hormuz (Figure 1) prevents the long-period swells from the Arabian Sea entering the Gulf. However, interaction between young swells/wind seas generated on

either side of the Strait of Hormuz and the complex bottom topography may produce complex wave conditions near the Gulf entrance. The impact of such interaction may be minor as far as the wave climate of the central Gulf is concerned. When the Sea of Oman is treated as a closed boundary in the wave model, the results indicate that waves coming from the Sea of Oman refracts and decays significantly around the Strait of Hormuz (Moeini et al., 2013). Therefore, waves within the Gulf are predominantly wind seas. The mean wave periods (T_m) are also reported to be between 1.5 and 5.0 s (Li et al., 2020). Waves in the central Gulf are influenced by winds from both NW and SE, however, dominated by NW winds (Vieira et al., 2020). It has been identified that more energetic areas in the Gulf are in the southern region (off Dubai), where the extreme (99th percentile) significant wave height (H_s) is greater than 2.7 m and peak wave period (T_p) is about 8.0 s during shamal dominated conditions. The seasonal mean H_s in the Gulf is higher during winter (upto 0.8 m) than other seasons (Kamranazad, 2018). The Bahrain and Qatar peninsulas cause sheltering effects on the predominant northwesterly waves, thus significant reduction in H_s occurs along the southwest and east coast of Qatar (Vieira et al., 2020). Liao and Kaihatu (2016a) pointed out that the refraction causes 20% total energy deviation (TED) along the north-eastern corner of Qatar during winter. In Doha Bay, the waves from NW are under fetch-limited conditions, which result in low wave heights (Liao and Kaihatu, 2016b). Moreover, occasionally developed easterly waves with relatively higher H_s were identified along the east coast of Qatar.

Although previous studies provide a brief overview of the wave conditions in the Gulf, the systematic variations in wave parameters in the EEZ of Qatar due to different wind systems are yet to be unravelled. The present study aims at exploring the wave variabilities by analysing measured wave parameters off Fuwairit, north coast of Qatar and numerical wave model results within the EEZ of Qatar obtained from CMEMS (Copernicus Marine Environment Monitoring Service). Fuwairit is a coastal village in Qatar, located in the municipality of Ash Shamal, approximately 90 km north of Doha. Fuwairit has a long stretch of beach with fine and white sand. It is an important site for Qatar's oil industry, and coral reefs are not far from the measurement site. It is a popular camping spot and a favourable site for kite surfers who come here on windy days. Fuwairit coastal area is exposed to the central Gulf, influenced by different wind, wave and current systems and in the proximity to the dynamics of the central Gulf. The deployment of oceanographic equipment was carried out as a part of the ongoing physical oceanographic investigations in this region.

2. Data and methods

Waves measured off Fuwairit (Figure 1), north coast of Qatar has been analyzed in this study. The measurements have been carried out using Seaguard Recording Current Meter (RCM) and Signature

1000 Acoustic Doppler Current Profiler (ADCP) placed within a horizontal distance of 150 m distance between them. The wave data were sampled at every 10 minutes interval. The RCM was moored 2m above the seabed during 29 October – 26 November 2019, while the ADCP was deployed in the seabed for a short period (29 October – 01 November 2019). The water depth in the measurement location is 7.0 m.

We processed the non-directional wave parameters H_s and T_p , from the RCM, while the directional wave parameters H_s , T_p and mean wave direction (MWD) have been obtained from the ADCP. Although the duration of measured data is short, we find that the non-directional wave parameters measured using ADCP are consistent with those obtained from RCM. Moreover, MWD obtained from the ADCP has been used for the verification of wave direction obtained from reanalysis data as no other measured wave data could be obtained to incorporate in this study. The accuracy of the pressure sensor in the RCM is 0.04% of the Full-Scale Output (FSO) (<https://www.aanderaa.com/media/pdfs/SeaGuard-RCM-Basic.pdf>). The accuracies of H_s and MWD in the ADCP are <1% of measured value and 2° , respectively (<https://www.nortekgroup.com/export/pdf/Signature1000.pdf>).

The European Centre for Medium-Range Weather Forecasts (ECMWF) provide hourly estimates of a large number of atmospheric, land and oceanic climate variables through their Reanalysis v5 (ERA5) (Hersbach et al., 2019). A larger quantity of past observations has been assimilated into the global estimate to ensure quality of the ERA5 product. The spatial grid resolution of ERA5 winds is 30 km. The ERA5 winds have a better accuracy compared to its predecessor ERA-Interim (Rivas and Stoffelen, 2019). The ERA5 winds were validated with in-situ measurements in the Gulf (Mahmoodi et al., 2019) as well as along the east coast of Qatar (Aboobacker et al., 2020a). We used the ERA5 winds in the present study to characterize the winds in the EEZ of Qatar.

The CMEMS provides 3-hourly global analysis and forecast waves in $0.083^\circ \times 0.083^\circ$ (~ 9 km) resolution driven by the winds from the ECMWF Integrated Forecasting System (IFS, 6-hourly analysis and 3-hourly forecast). The CMEMS also provides 3-hourly reanalysis waves in $0.2^\circ \times 0.2^\circ$ resolution (~ 22 km) driven by the ERA5 winds. The CMEMS uses Météo-France wave model (MFWAM) incorporating the ECWAM-IFS-38R2 computing code with dissipation terms developed by Ardhuin et al. (2010), where, the model mean bathymetry is generated by using ETOPO2 (National Geophysical Data Center, 2006). The wave spectrum is discretized in 24 directions and 30 frequencies starting from 0.035 Hz to 0.58 Hz. In this study, both 9 km and 22 km resolution wave model outputs (during Jan 2019 – April 2020) have been used to characterise the waves in the EEZ

of Qatar. The wave measurement location (off Fuwairit) falls in a dry grid in 9 km resolution model, while it falls in a wet grid in 22 km resolution model. Thus, the validation of the CMEMS waves has been carried out using the latter. However, being relatively fine resolution, we used the 9 km resolution outputs for a spatial analysis. We find no significant difference among both the wave model results, when the results are compared at an offshore location within the EEZ of Qatar (comparison is not shown). It is worthy to note that the temporal and spatial resolutions of the CMEMS waves are adequate to describe the effects of regional wind systems on waves in the Gulf. However, such resolutions may not capture the effects of waves generated by the local sea/land breezes.

3. Results and discussion

3.1 Wind climate in the EEZ of Qatar

The Qatar peninsula and the offshore experience winds from various directions. The northwesterly/north-northwesterly (NW/NNW) winds are predominant along the north coast of Qatar throughout the year, in which the shamal winds are dominant (Figure 2). Their relative contribution is higher during winter (November – April) than summer (May – October). The easterly to south-southeasterly (E to SSE) winds are more pronounced in winter, which are influenced by the large-scale NE monsoon winds. In addition to regional winds, local breezes are also found throughout the year in significant proportion. Sandeepan et al. (2018) identified sea-land breeze systems in Qatar, which causes diurnal variability in wind speeds, especially in the onshore regions. The percentage occurrence of winds off Fuwairit is the highest from NNW (23.1%), followed by NW (17.7%) and N (7.8%), while the lowest is from SW (1.7%).

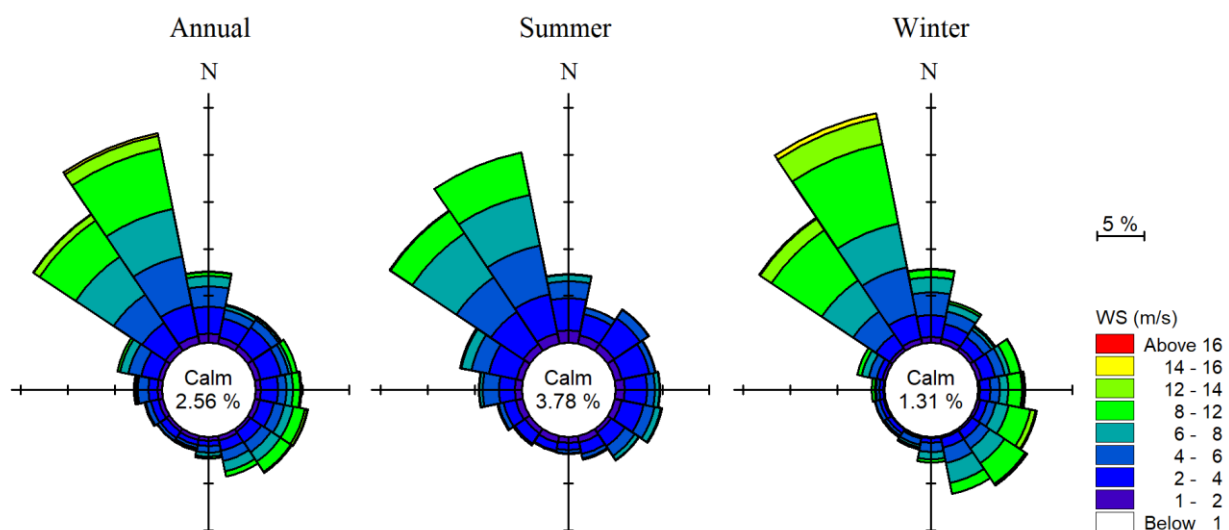


Figure 2. Annual, summer and winter wind rose diagrams off Fuwairit during 2019

In an annual cycle, the wind speeds show high variability during winter driven by shamal and easterly winds (Figure 3). Aboobacker et al. (2020a) showed that the monthly mean wind speeds along the north coast of Qatar are the highest during February and the lowest during September. The maximum wind speed of 16.3 m/s identified in the year in consideration was associated with a strong easterly wind system, occurred on 23 Mar 2019. This is a rare case when compared with the subsequent peaks in wind speeds, which are mostly from the NW/NNW directions. The percentage occurrence of high winds (above 10 m/s) is 8.6%, whereas that of moderate winds (between 5 and 10 m/s) 39.6% and low winds (below 5 m/s) 51.8%.

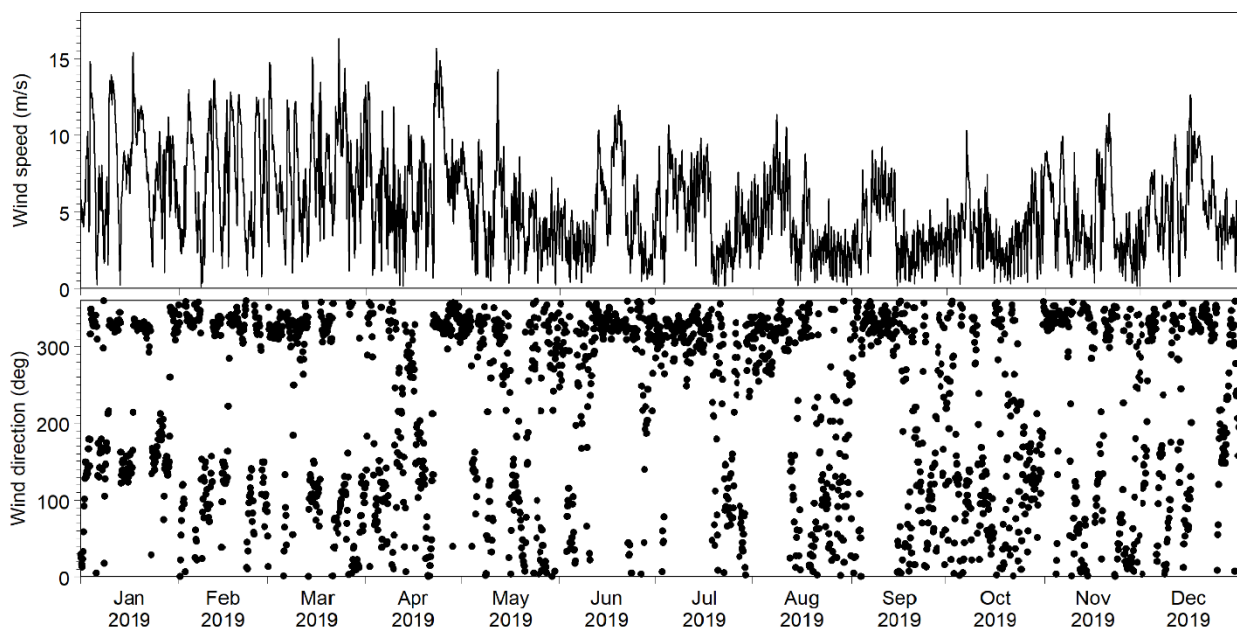


Figure 3. Time series of ERA5 wind speed and direction off Fuwairit during 2019

Figure 4 shows the snapshots of shamal and easterly winds in the EEZ of Qatar during the wave measurement period. Here, the shamal winds during the measurement period are predominantly from the NNW and of order of 8 – 12 m/s, with a decreasing intensity towards south. The typical speeds of shamal winds in the Gulf are generally 15 – 20 m/s (Senafi and Anis, 2015), while a maximum speed of 22 m/s were identified within the last 40 years (Aboobacker et al., 2020b). The annual occurrence of winds from the directional sector NW-N is around 49%. The easterly winds in the EEZ during the measurement period are typically of the order of 4 – 8 m/s, decreasing towards the land areas. Although the occurrence is relatively low (less than 16% from the directional sector ENE-ESE), the easterly winds have high potential, considering a longer fetch (350 – 450 km) in the central and southern Gulf, and hence, their impact along the east coast of Qatar.

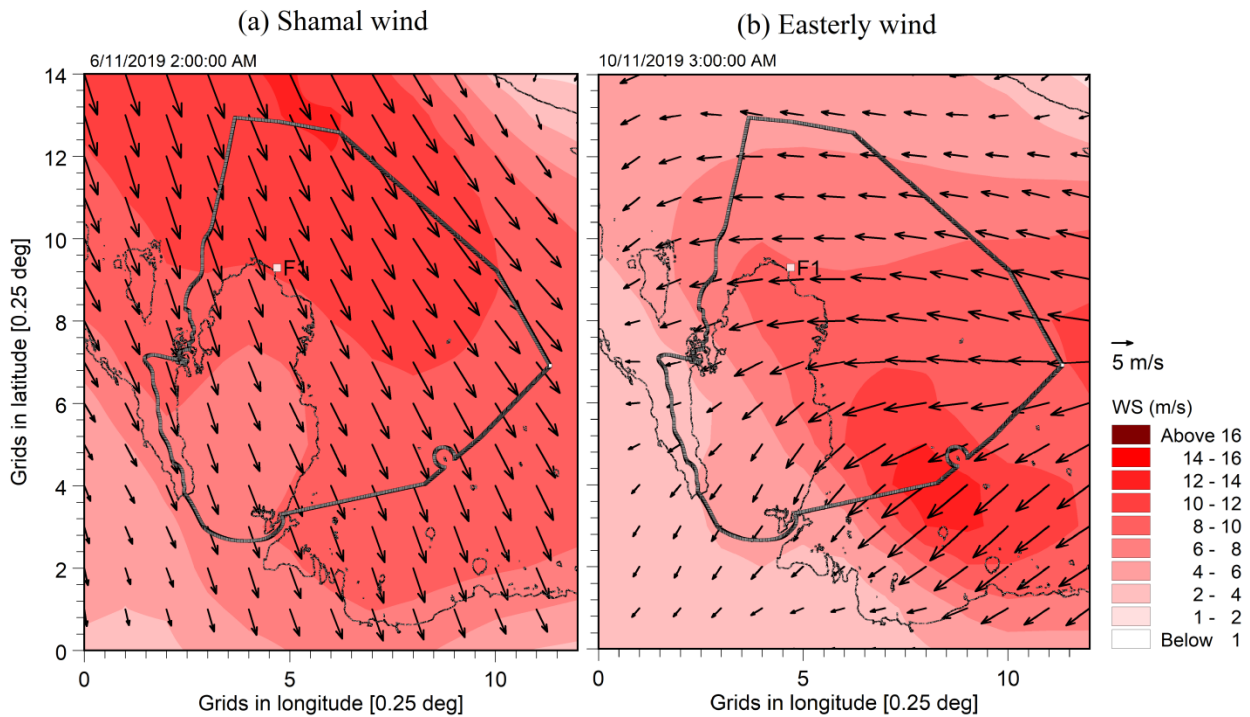


Figure 4. Snapshots of wind patterns in the EEZ of Qatar during the wave measurement period representing (a) shamal winds and (b) easterly winds.

3.2 Observed variations in wave parameters

There are typically two high wave conditions off Fuwairit, which are associated with (i) shamal winds and (ii) easterly winds (Figure 5). During the measurement period, three shamal events (namely, Shamal I: 31 October – 02 November, Shamal II: 05 – 07 November and Shamal III: 20 – 21 November) and two easterly wind events (Easterly I: 10 – 11 November and Easterly II: 16 – 18 November) were identified. The wind speeds during the pre-shamal period were generally low and the directions were between E and S. However, during the active shamal events, the H_s and T_p gradually increased in response to the increase in shamal wind speed. In addition, a gradual shift of wave direction from E to NNW/NW has been noticed. The maximum H_s measured during Shamal I, Shamal II and Shamal III events are 1.23 m, 1.32 m and 1.12 m, respectively, while the maximum T_p are 6.3 s, 6.7 s and 5.7 s, respectively. The maximum H_s measured during Easterly I and Easterly II events are 1.38 m and 1.68 m, respectively, while the maximum T_p are 6.5 s and 6.9 s. This indicates that the H_s of easterly waves are higher than the shamal induced waves along the north coast of Qatar during the measurement period. This is because of the longer fetch available for the easterly waves, while the fetch of shamal induced waves is very limited considering the proximity of the measurement location to the coast and geographical orientation of the coastline. It is also obvious

that the month November exhibits a relatively low potential shamal wind speeds compared to the peak winter shamals (January-March) and summer shamals (June).

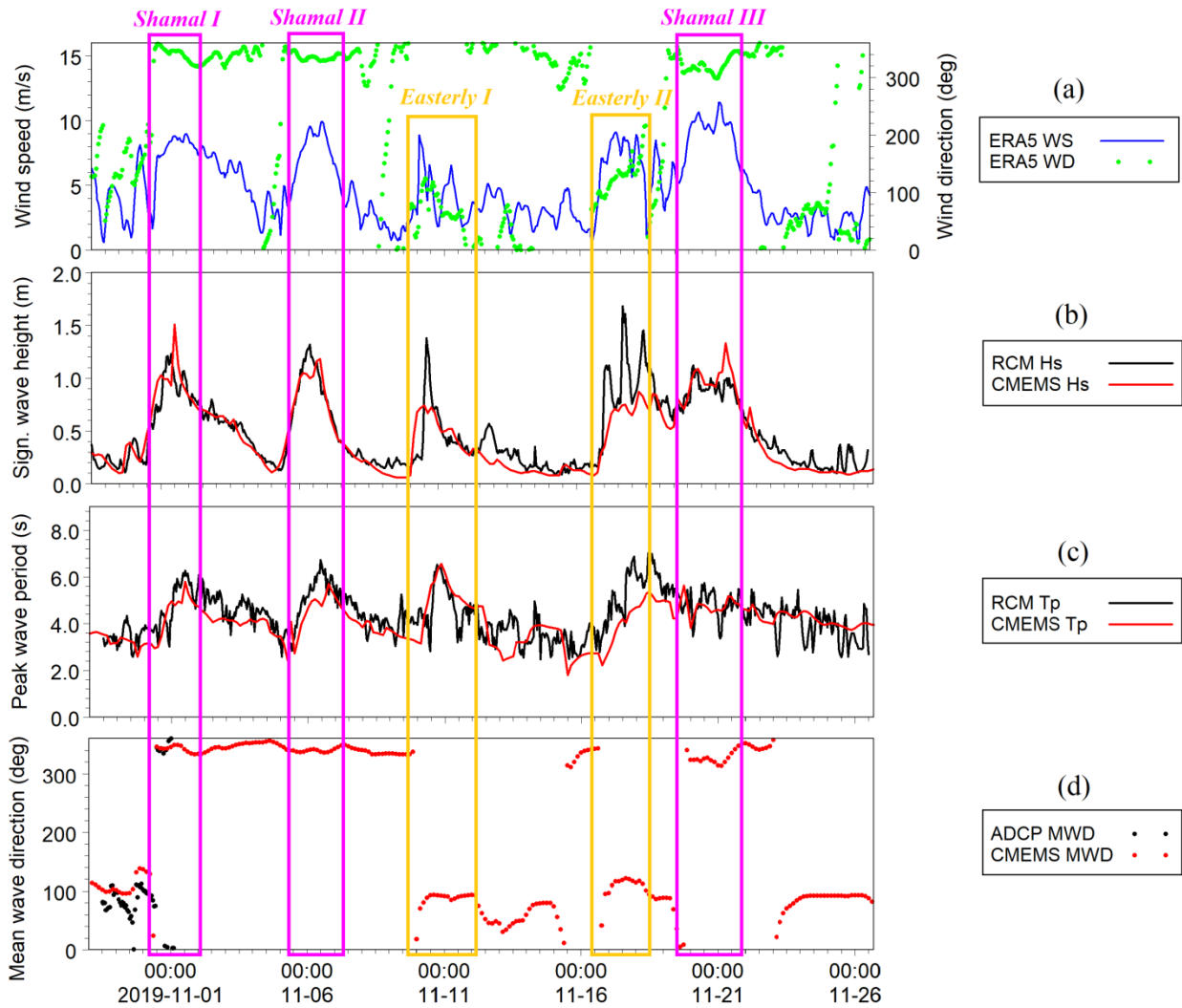


Figure 5.(a) ERA5 wind speed and direction, (b) H_s from RCM and CMEMS, (c) T_p from RCM and CMEMS and (d) MWD from ADCP and CMEMS.

3.3 Verification of CMEMS wave parameters

Wave parameters obtained from the CMEMS have been compared with the measurements off Fuwairit (Figure 5b-d). The comparison shows that the CMEMS wave parameters match reasonably well with the measurements. For easterly waves, H_s and T_p are under-estimated as shallow water processes are not well executed in the coarse model grid (~22 km resolution), which is a matter of concern for the shore normal propagating waves. Shamal waves are in the NNW direction, which have a long fetch towards offshore until it reaches the UAE coast. Thus, in the measurement area, it has a relatively lower attenuation compared to a shore normal propagating wave. This resulted in a

reasonably well comparison for waves in CMEMS model during peak shamal conditions. The correlation coefficient, bias, root mean square error (r.m.s.e.) and scatter index between the measured and model H_s are 0.88, -0.05 m, 0.17 m and 0.35, respectively. The CMEMS T_p is slightly underestimated. The correlation coefficient, bias, r.m.s.e. and scatter index between the measured and model T_p are 0.68, -0.29 s, 0.77 s and 0.18, respectively. The MWD obtained from the CMEMS data matches reasonably well with that of ADCP data within the limited data duration, especially the directional shift associated with different wind systems has been well-captured. Ravdas et al. (2018) observed a good overall performance of CMEMS wave parameters in regional seas and our results are in consistent with their work. Thus, we used this dataset to derive a qualitative description on the annual and seasonal variations of waves along the north coast of Qatar.

3.4 Spatial patterns of shamal and easterly waves

Shamal waves are the strongest waves in the Gulf with significant spatial variations. Figure 6 shows the snapshots of the shamal waves in the Gulf during 01-02 Mar 2019. When the shamal wind prevails, the height of the NW waves increases in the northern Gulf, while the pre-existing waves (NE to SW) in the southern Gulf retreats. Depending on the intensity and duration of shamal winds, the shamal waves are further evolved and propagated up to the southern Gulf, which often cross the Strait of Hormuz. In a previous study, Aboobacker et al. (2011) identified the shamal winds and waves prevailing in the Sea of Oman and the Arabian Sea. The north and northeast boundaries of the EEZ of Qatar experiences higher shamal waves, H_s of the order of 3.4 m in this case. However, the highest shamal waves could be observed in the southern Gulf, especially off the west coast of UAE with H_s of the order of 3.8 m. This is in consistent with the findings of Vieira et al. (2020). Along the coast of Qatar, the shamal waves are typically in the NNW direction. The west and southeast coasts of Qatar experiences relatively lower shamal waves ($H_s < 2.0$ m) due to topographical features as well as fetch limitations.

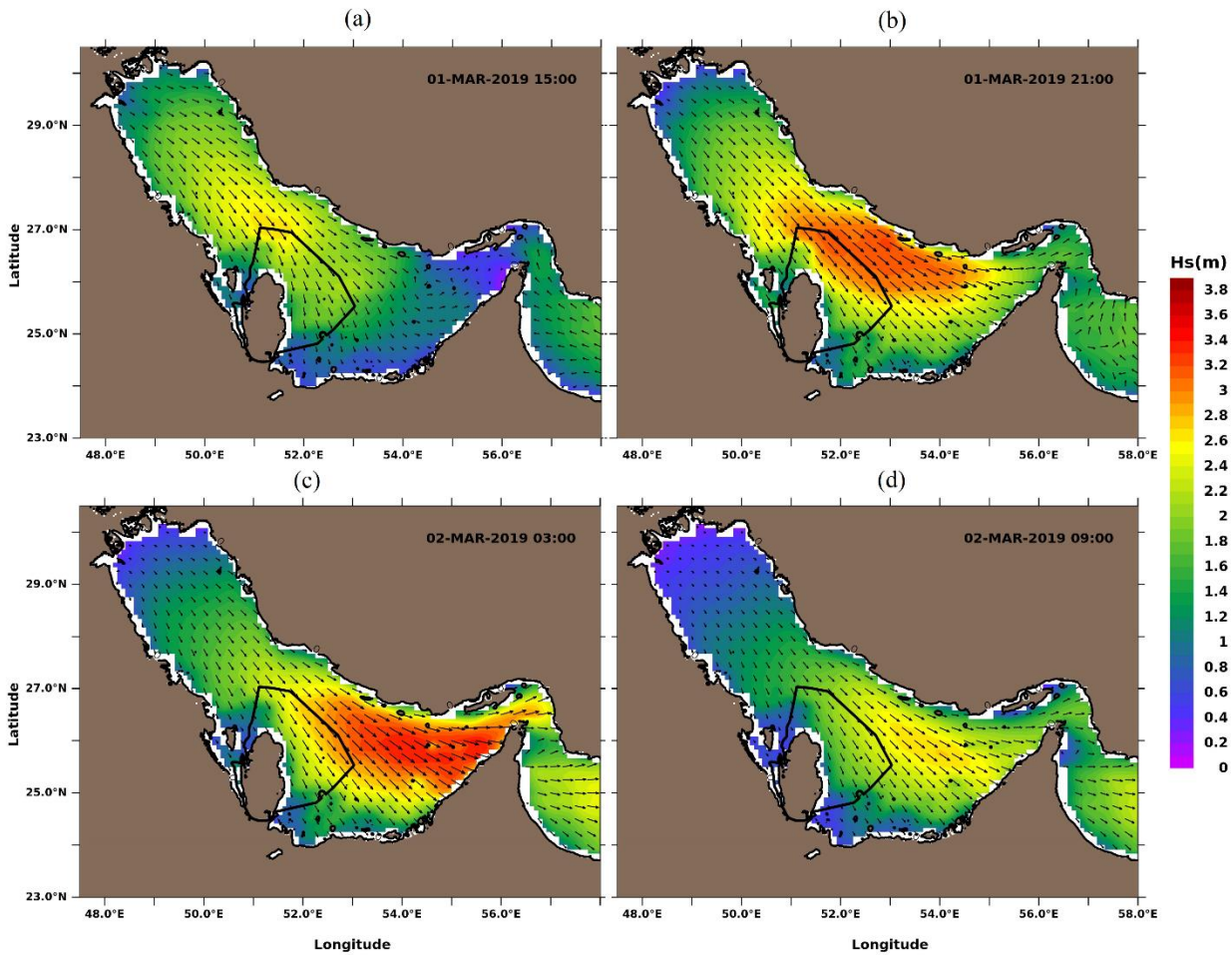


Figure 6. Spatial distribution of shamal induced waves in the Gulf during 01-02 Mar 2019: (a) 15 h, (b) 21 h, (c) 03 h and (d) 09 h.

The timeseries of wave parameters off Fuwairit extracted from CMEMS for the year 2019 indicate that there are several peaks with H_s higher than 1.5 m (Figure 7). The associated peak wave periods are between 6.0 and 8.5 s. Most of these peaks are from the NNW, while a few are from the E. The higher NNW waves are due to shamal winds, while the higher E waves are due to easterly wind events. The shamal induced maximum H_s is 2.12 m and the corresponding T_p is 7.0 s. The easterly winds are either due to the NE monsoon winds or by the Nashi winds (Villiers and Heerden, 2011). The Nashi winds are the stronger, dusty and dry northeasterly winds originating from Iran during winter, which enter into the Gulf through the southern coast of Iran (near the Strait of Hormuz) as northeasterlies. These winds further flow as easterlies during their propagation in the central Gulf and as southeasterlies in the northern Gulf. The mechanism of the formation of Nashi winds in Iran are similar to that of South Asian Subtropical Low-Level Jet identified near the Iranian borders of the Afghanistan and Pakistan (Anoop et al., 2019), as they are in conjunction with each other. The easterly winds in the Gulf are often modified by the influence of low-pressure systems developed over the

Mediterranean and the northern Arabian Peninsula. The highest H_s ($=2.3$ m, off Fuwairit) occurred on 25 Mar 2019 was due to such easterly event, during which the T_p was around 8.0 – 8.5 s. This indicates that the north coast of Qatar experiences large waves from the east, although their occurrences are relatively low. Dry and warm southeasterly winds, namely Kaus, with moderate speeds are also observed in the Gulf during winter (Rao et al., 2001). The wave rose plot (Figure 8) clearly depicts the impact of these wind systems (shamal, Nashi and Kaus) on wave generation in the Gulf, especially along the north coast of Qatar. The occurrence of higher waves due to these wind sources is more during winter than summer. A few wave systems with lower H_s are also found from various directions, some of which may be attributed to sea-land breezes identified within the EEZ of Qatar (Sandeepan et al., 2018).

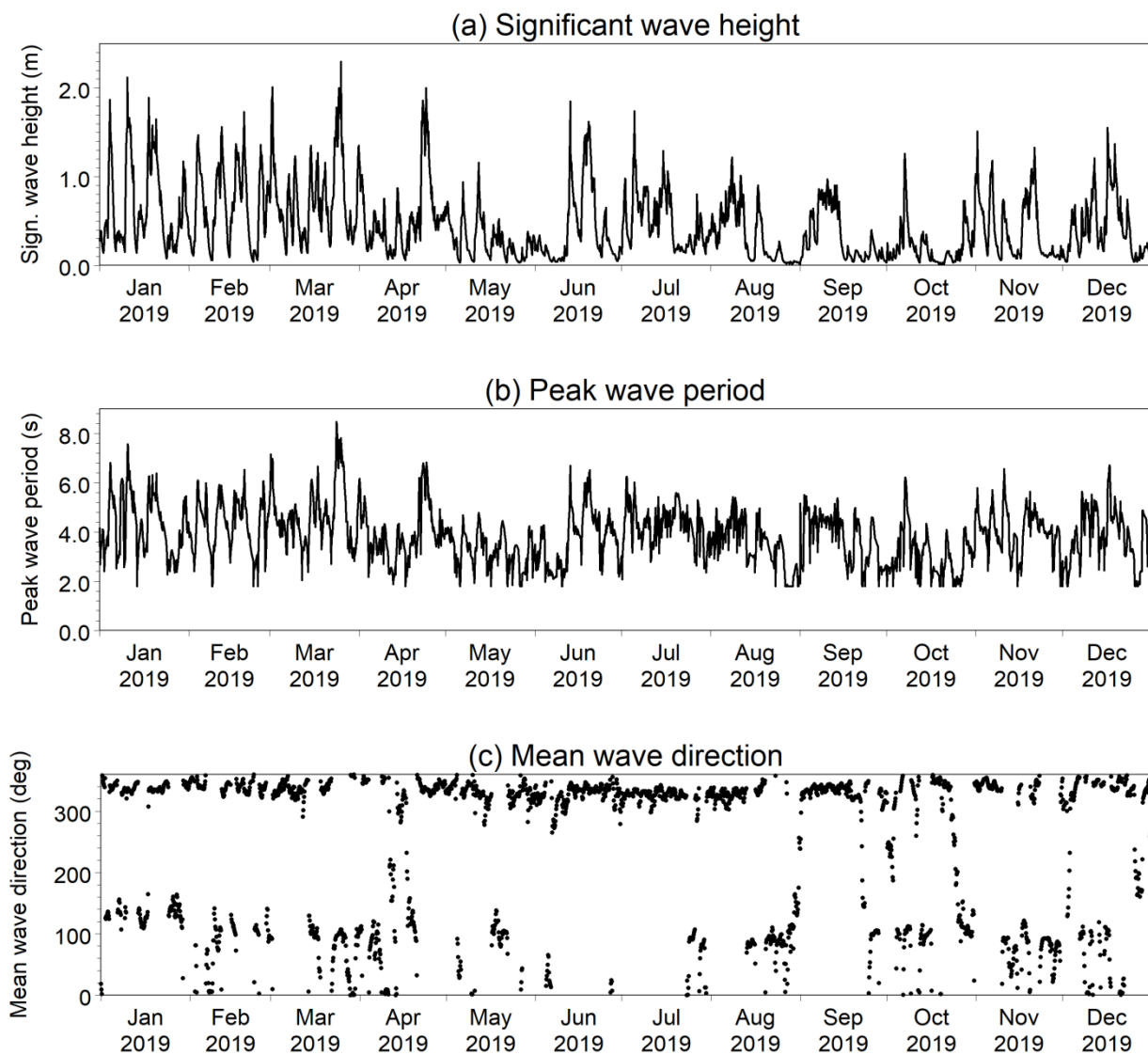


Figure 7. Time series of CMEMS wave parameters off Fuwairit during 2019: (a) significant wave height, (b) peak wave period and (d) mean wave direction

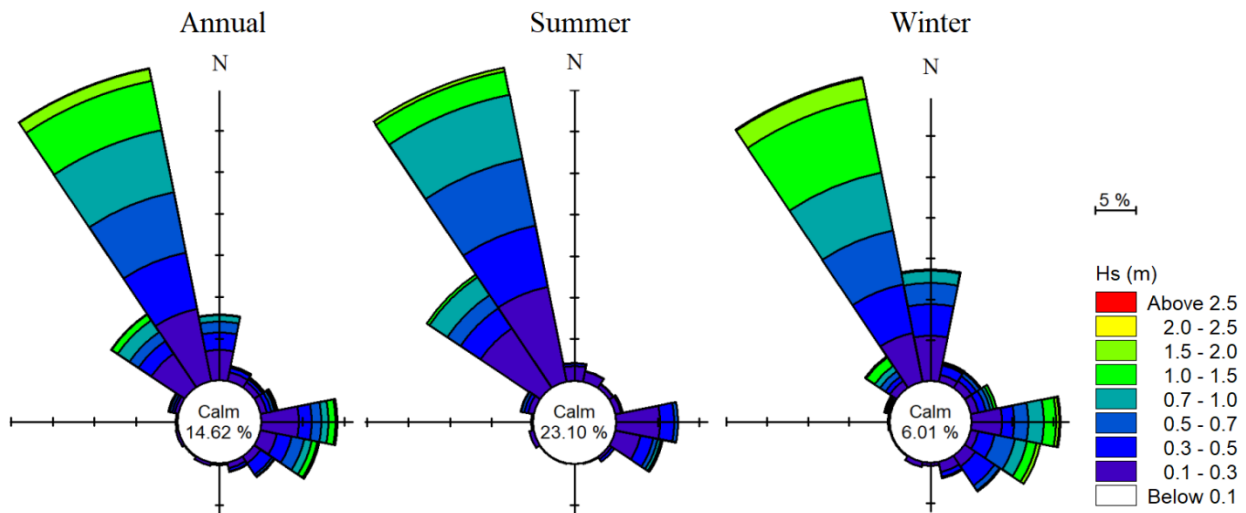


Figure 8. Annual, summer and winter wave roses off Fuwairit

Figure 9 shows the snapshots of the wave vectors during an easterly wind event. The early generation of easterly waves is near the Strait of Hormuz within the limited fetch, resulting in relatively small H_s , of the order of 1.0 – 1.8 m (Figure 9a). As the fetch expands and wind intensity increases, the central and northern Gulf dominate with higher H_s , of the order of 3.3 m and 3.8 m, respectively (Figure 9b-d). In comparison with shamal waves (Figure 6), the easterly waves have higher H_s along the east coast of Qatar (upto 2.6 m), although their relative occurrence is low. The processes occurring in the nearshore regions are not only by the waves, but also by the currents induced by the tide-driven flows and regional scale circulations. These will have significant implications in physical and biogeochemical processes along the east coast of Qatar. A more quantitative assessment of winds and waves using fine resolution models such as WRF and SWAN, respectively are required to capture the local effects to a good extent and thus, to enhance the understanding of biogeochemical interactions.

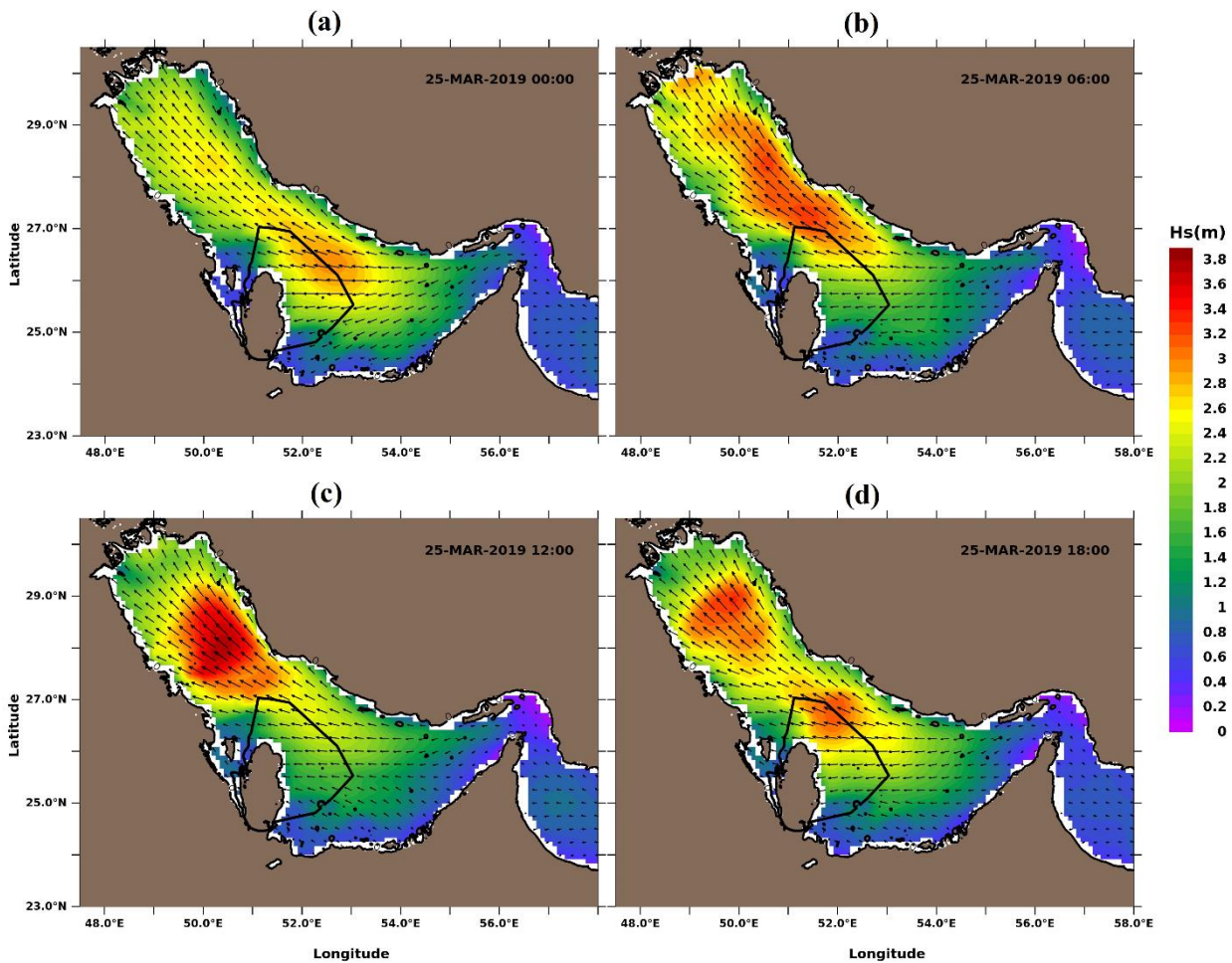


Figure 9. Spatial distribution of easterly waves in the Gulf on 25 Mar 2019: (a) 00 h, (b) 06 h, (c) 12 h and (d) 18 h.

3.5 Annual, seasonal and monthly distribution of H_s in the EEZ of Qatar

3.5.1 Annual mean and maximum

The annual mean H_s in the EEZ of Qatar is of the order of 0.2 – 0.7 m, where the highest waves are observed in the northeast offshore boundary (Figure 10a). Earlier studies reported that the long term highest mean H_s in the Gulf is along the central strip of the Gulf, that includes the north and northeast boundaries of the EEZ of Qatar (Kamranazad, 2018; Mahmoodi et al., 2019). The west and southeast coasts of Qatar have lower H_s (< 0.4 m) due to shallow depths and shielding orography of the peninsular Qatar and Bahrain in the central Gulf, which attenuate/prevent large waves entering in these regions. The annual mean H_s and T_p off Fuwairit are 0.46 m and 3.9 s, respectively. This indicates that northern coast of Qatar experiences short-period waves with moderate heights during most part of the year.

The annual maximum H_s in the EEZ of Qatar ranges between 1.0 m and 3.3 m (Figure 10b). The highest values are observed in the eastern boundary of EEZ. This is consistent with the distribution of shamal waves, where the highest waves are found in the southern Gulf (Figure 6c). This indicates that the eastern boundary of the EEZ experiences higher waves due to shamal winds, while the east coast of Qatar experiences higher waves due to easterly winds (Figures 5b and 6a). The annual maximum H_s and $T_{p\text{off}}$ Fuwairit are 2.3 m and 8.5 s, respectively.

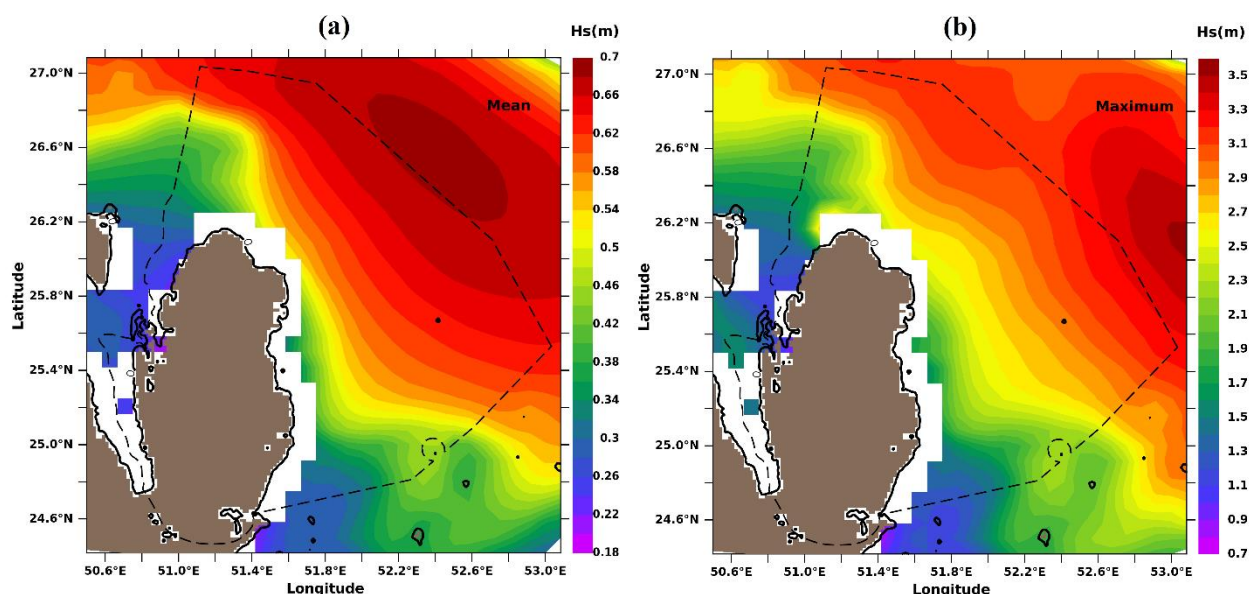


Figure 10. The (a) mean H_s and (b) maximum H_s in the EEZ of Qatar during 2019

3.5.2 Seasonal mean

Waves in the Gulf are higher during winter than summer (Hubert et al., 1983). We found similar inferences in the seasonal mean H_s in the EEZ of Qatar (Figure 11). The winter mean H_s is high in the northeastern offshore boundary of the EEZ, ranging up to 0.76 m, whereas the summer mean H_s is high in the northern offshore boundary of the EEZ, ranging up to 0.56 m. Kamranazad (2018) identified that the H_s hotspots are in the central Gulf during winter shamal, while they move to the northwest region during summer shamal. Shifting of these hotspots is reflecting in the seasonal mean H_s in the EEZ of Qatar.

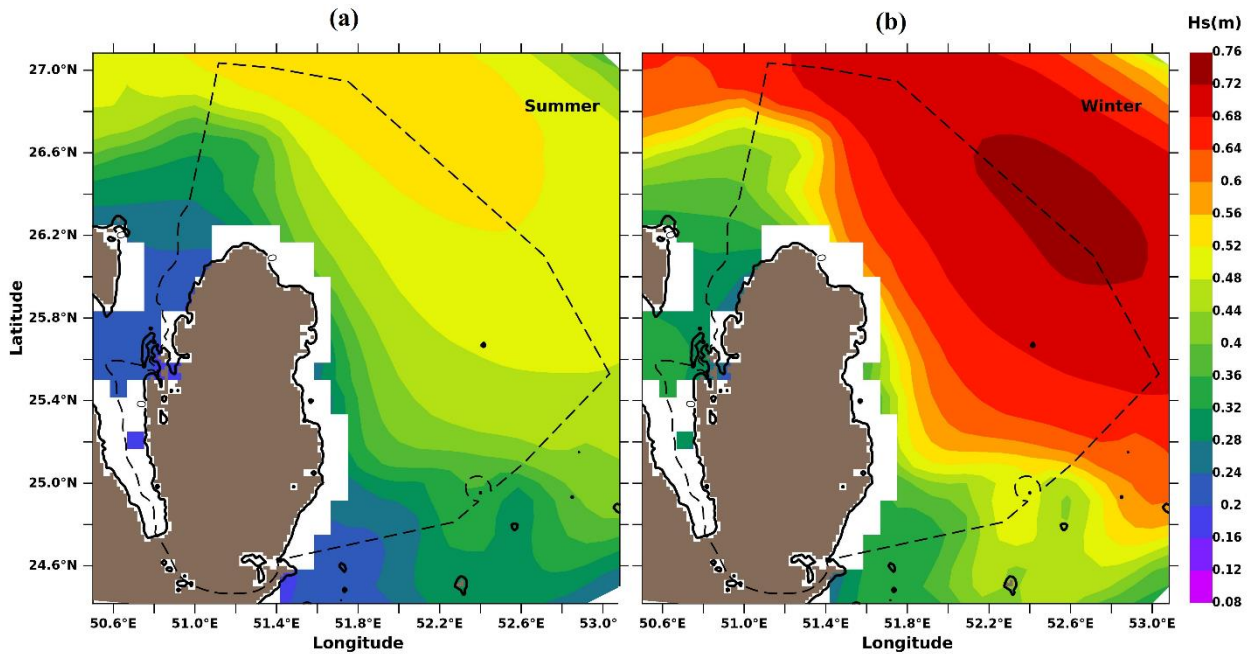


Figure 11. The seasonal mean H_s in the EEZ of Qatar: (a) summer (May – Oct 2019) and (b) winter (Nov 2019 – Apr 2020).

3.5.3 Monthly mean

The highest monthly mean H_s in the EEZ of Qatar occurs during March (upto 1.20 m), followed by February (upto 1.06 m) and January (upto 0.96 m) (Figure 12). However, this may not be consistent when compared with a long-term average in the Gulf, where the highest monthly mean H_s occurs during February (Kamranazad, 2018). We find exceptional high easterly waves during March 2019 due to strong Nashi winds, which caused an increase in the mean H_s compared to other months. The relatively higher mean H_s during March 2019 was not observed in the adjacent years (2018 and 2020). There exists a spatial variability in the higher mean H_s during January – March; i.e., the highest value during January is in the northern offshore boundary, while that during February and March are in the northeastern offshore boundary of the EEZ. The spatio-temporal variations in mean H_s in the Gulf are subject to corresponding changes in the winds, especially the shamal and easterly winds prevailing during these months. A long-term analysis on Nashi and shamal winds is required to understand their spatio-temporal variabilities and the associated changes in the waves in the Gulf and the EEZ of Qatar.

April and June exhibit mean H_s upto 0.86 m and 0.71 m, respectively, in the northeastern offshore boundary, while July exhibits upto 0.81 m in the northern offshore of the EEZ. In other months, the mean H_s within the EEZ is less than 0.60 m. The lowest monthly mean H_s is observed during

October. The nearshore processes are not well executed in the given results because of the relatively coarser spatial resolution of the model. The wave attenuation due to coral beds, seagrass meadows and mangroves should be given particular attention in the EEZ of Qatar. Several other factors may also influence the nearshore wave characteristics, particularly the effect of opposing winds and currents. A far detailed analysis considering the above aspects is planned in our future work.

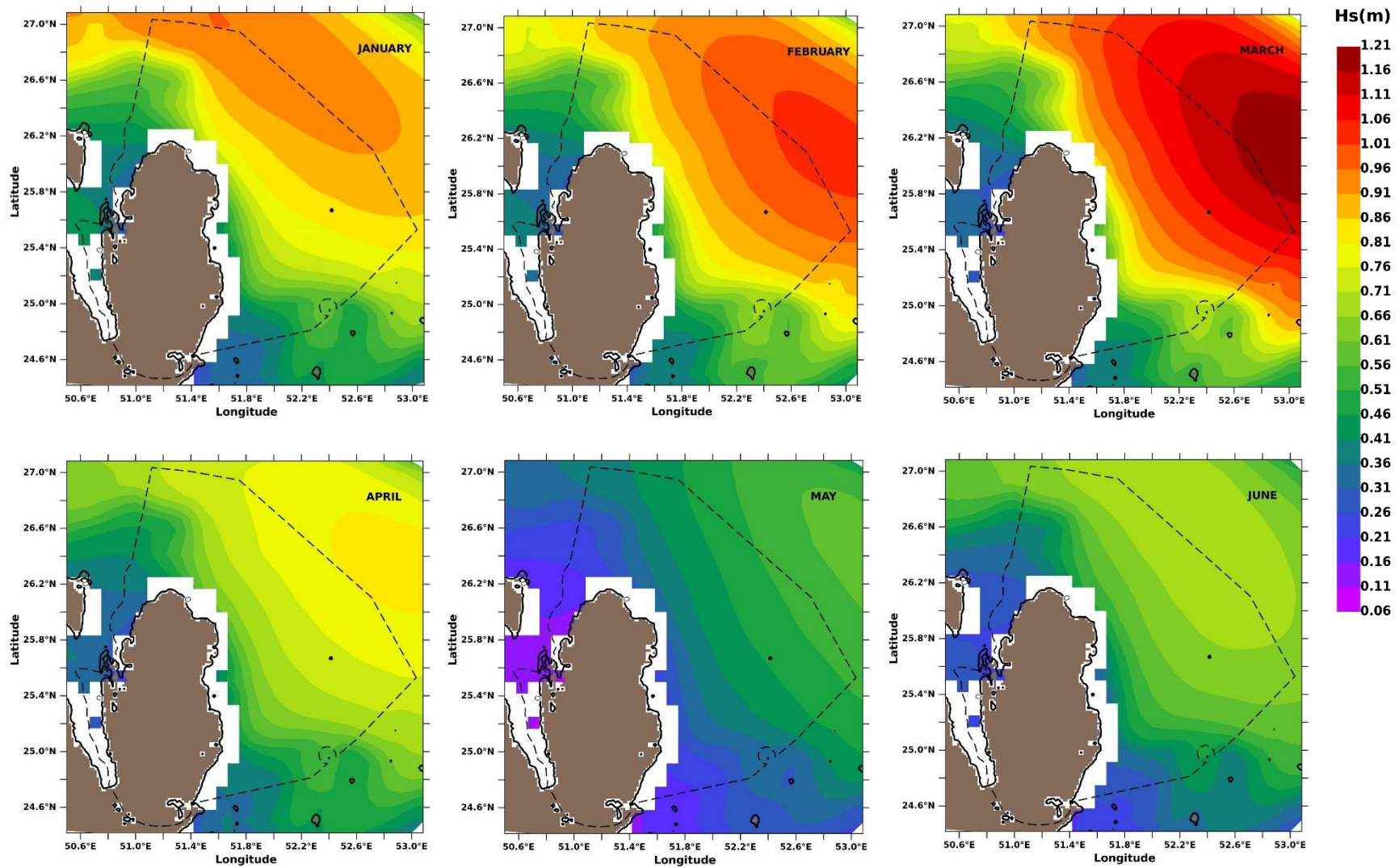


Figure 12. The monthly mean H_s in the EEZ of Qatar during 2019.

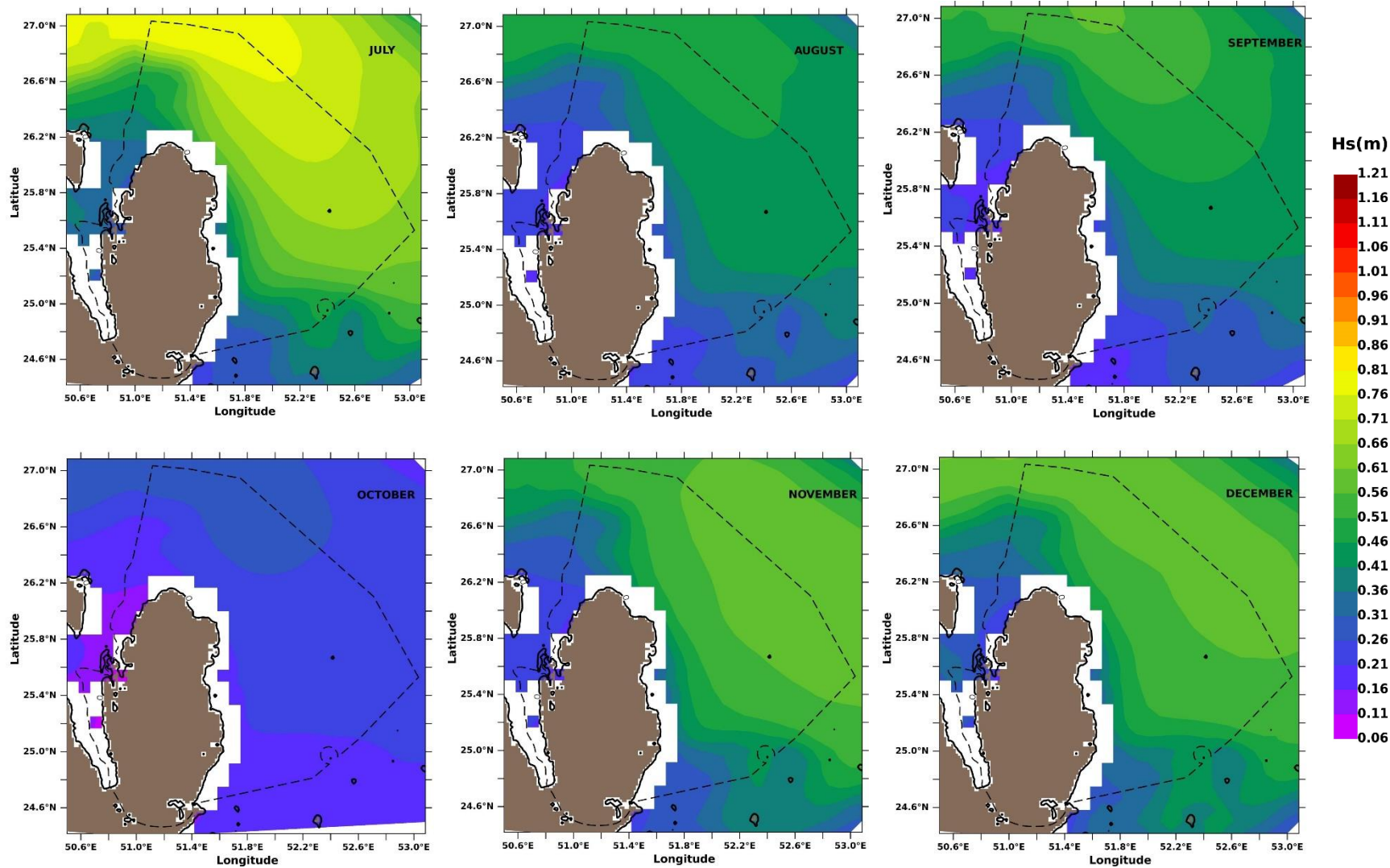


Figure 12 (continued).

4. Conclusions

The wave characteristics in the EEZ of Qatar are analysed using the measured waves off Fuwairit (at 7 m depth) and the reanalysis waves obtained from CMEMS. The CMEMS waves have been validated for the first time in the Arabian/Persian Gulf and the model waves reasonably reproduced the waves off Fuwairit. The results indicate that the easterly waves generated due to Nashi winds influence the east and northeast coasts of Qatar in a relatively higher potential than that during shamal events. However, the shamal waves show clear dominance in the northern and northeastern offshore boundaries of the EEZ of Qatar. These discrepancies are attributed to: (i) the shamal waves have fetch limitations within the east and northeast coast of Qatar, while the easterly waves have sufficient fetch, of the order of 350 – 450 km, to dominate over the shamal waves and (ii) the northern and northeastern offshore boundaries of the EEZ of Qatar are in the central strip of the Gulf, which are highly exposed to strong shamal winds with relatively longer fetch. The annual mean and maximum H_s off Fuwairit are 0.46 m and 2.3 m, respectively, while those in the northern/northeastern boundary of the EEZ are 0.7 m and 3.3 m, respectively. Seasonally, the winter exhibits higher H_s than summer with a hotspot in the northeastern boundary, while the hotspot during summer is in the northern boundary of the EEZ. We find exceptional easterly waves during March 2019 contributing to the highest monthly mean H_s - a deviation from the long-term analysis, which is due to relatively stronger Nashi winds over the Gulf during this month.

Although the role of major wind systems on the waves in the Gulf has been examined, the interaction of multi-directional and multi-frequency waves, including those generated due to sea/land breezes and associated changes in the resultant waves, need to be explored. This can be done through spectral analysis; however, the availability of measured spectral waves is a limiting factor to carry out such analysis in this work. Future study is planned to unravel the spectral behaviour of the waves within the EEZ of Qatar using fine scale spectral wave modelling.

Acknowledgments

We thank Prof. Hamad Al-Saad Al-Kuwari, Director, Environmental Science Center, Qatar University for his constant encouragement and support. We acknowledge Director, CSIR-NIO, Goa for his support in this study. We are grateful to Mr. Mehmet Demirel, Mr. Reyniel Gasang, Mr. Faisal Al-Quaiti and Mr. Mark Chatting for their assistance during the data collection. This

work was jointly carried out under the IRCC International Research Co-Fund Collaboration Program of QU and CSIR-NIO, executed through ORS, QU (IRCC-2019-002). The NIO contribution number for the author from CSIR-NIO is xxxx.

References

Aboobacker, V.M., Shanas, P.R., Veerasingam, S., Ibrahim M.A.S. Al-Ansari, Fadhil N Sadooni, Vethamony, P., 2020a: Long-term assessment of onshore and offshore wind energy potentials of Qatar. *Energies* (In Press).

Aboobacker, V.M., Shanas, P.R., Al-Ansari, E.M.A.S, Sanil Kumar, V., Vethamony, P., 2020b. The maxima in northerly wind speeds and wave heights over the Arabian Sea, the Arabian/Persian Gulf and the Red Sea derived from 40 years of ERA5 data. *Climate Dynamics*. <https://doi.org/10.1007/s00382-020-05518-6>.

Aboobacker, V.M., Vethamony, P., Rashmi, R., 2011. “Shamal” swells in the Arabian Sea and their influence along the west coast of India. *Geophysical Research Letters* 38, L03608. <https://doi.org/10.1029/2010GL045736>.

Anoop, T.R., Unnikrishnan, C.K., Ashok, K., Ramachandran, K.K., Prakash, T.N., 2019. South Asian subtropical low-level jet: influence on regional hydrology and aerosol optical depth. *Current Science* 117, 852-858. <https://doi.org/10.18520/cs/v117/i5/852-858>.

Ardhuin, F., Magne, R., Filipot, J.-F., Van der Westhuyzen, A., Roland, A., Quefeulou, P., Lefèvre, J.M., Aouf, L., Babanin, A., Collard, F., 2010. Semi empirical dissipation source functions for wind-wave models: Part I, definition and calibration and validation at global scales. *Journal of Physical Oceanography* 40, 1917-1941. <https://doi.org/10.1175/2010JPO4324.1>.

Hubert, W. E., Morford, D. R., Hull, A. N., Englebretson R. E., 1983. *Forecasters Handbook for the Middle East/Arabian Sea*. Naval Environ. Predict. Res. Facil., Monterey, Calif.

Kamranzad, B., 2018. Persian Gulf zone classification based on the wind and wave climate variability. *Ocean Eng.* 169, 604-635. <https://doi.org/10.1016/j.oceaneng.2018.09.020>

Kamranzad, B., Etemad-shahidi, A., Chegini, V., 2013. Assessment of wave energy variation in the Persian Gulf. *Ocean Eng.* 70, 72–80. <https://doi.org/10.1016/j.oceaneng.2013.05.027>.

Khan, N.Y., Munawar, M., Price, A. R. G., 2002. *The Gulf Ecosystem: Health and Sustainability*. Backhuys Publishers, Leiden, pp. 509. <https://doi.org/10.14321/j.ctt1tm7jkg>.

Hersbach, H., Bell, B., Berrisford, P., et al., 2019. Global reanalysis: goodbye ERA-Interim, hello ERA5. *ECMWF Newsl* 159, 17–24. <https://doi.org/10.21957/vf291hehd7>.

- Langodan, S., Cavaleri, L., Viswanadhapalli, Y., Hoteit, I., 2014. The Red Sea: a natural laboratory for wind and wave modelling. *J. Phys. Oceanogr.* 44, 3139-3159. <https://doi.org/10.1175/JPO-D-13-0242.1>.
- Li, D., Anis, A., Senafi, F.A., 2020. Physical response of the Northern Arabian Gulf to winter Shamals. *Journal of Marine Systems* 203, 103280. <https://doi.org/10.1016/j.jmarsys.2019.103280>.
- Liao, Y.P., Kaihatu, J.M., 2016a. Numerical Investigation of Wind Waves in the Persian Gulf: Bathymetry Effects. *J. Atmos. Ocean. Techno.* 33, 17-31.
- Liao, Y.P., Kaihatu, J.M., 2016b. The effect of wind variability and domain size in the Persian Gulf on predicting nearshore wave energy near Doha, Qatar. *Applied Ocean Research* 55, 18–36.
- Mahmoodi, K., Ghassemi, H., Razminia, A., 2019. Temporal and spatial characteristics of wave energy in the Persian Gulf based on the ERA5 reanalysis dataset. *Energy* 187, 115991. <https://doi.org/10.1016/j.energy.2019.115991>.
- Moeini, M.H., Etemad-Shahidi, A., Chegini, V., 2010. Wave modeling and extreme value analysis off the northern coast of the Persian Gulf. *Applied Ocean Research* 32, 209-218. <https://doi.org/10.1016/j.apor.2009.10.005>.
- National Geophysical Data Center, 2006. 2-minute Gridded Global Relief Data (ETOPO2) v2. National Geophysical Data Center, NOAA. <https://doi.org/10.7289/V5J1012Q>.
- Patlakhas, P., Stathopoulos, C., Flocas, H., Kalogeri, C., Kallos, G., 2019. Regional Climatic Features of the Arabian Peninsula, *Atmosphere* 10(4), 220. <https://doi.org/10.3390/atmos10040220>.
- Perrone, T.J., 1979. Winter shamal in the Persian Gulf, Naval Env. Prediction Res. Facility, Technical Report, 79-06, Monterey, 180pp.
- Pous, S., Lazouere, P., Carton, x., 2015. A model of the general circulation in the Persian Gulf and in the Strait of Hormuz: Intraseasonal to interannual variability. *Cont. Shelf. Res.* 94, 55-70. <https://doi.org/10.1016/j.csr.2014.12.008>.
- Rao, P.G., Al-Sulaiti, M., Al-Mulla A.H., 2001. Winter shamals in Qatar, Arabian Gulf. *Weather* 56, 444-451.
- Ravdas, M., Zakharioudaki, A., Korres, G., 2018. Implementation and validation of a new operational wave forecasting system of the Mediterranean Monitoring and Forecasting Centre in the framework of the Copernicus Marine Environment Monitoring Service. *Natural Hazards and Earth System Sciences* 18, 2675-2695. <https://doi.org/10.5194/nhess-18-2675-2018>.
- Rivas, M.B., Stoffelen, A., 2019. Characterizing ERA-Interim and ERA5 surface wind biases using ASCAT. *Ocean Sci* 15, 831–852. <https://doi.org/10.5194/os-15-831-2019>.

- Samiksha, S.V., Vethamony, P., Aboobacker, V.M., Rashmi, R., 2012. Propagation of Atlantic Ocean swells in the north Indian Ocean: a case study. *Nat Hazard Earth Sys.* 12, 3605-3615. <https://doi.org/10.5194/nhess-12-3605-2012>.
- Sandeepan, B.S., Panchang, V.G., Nayak, S., Krishnakumar, K., Kaihatu, J.M., 2018. Performance of the WRF Model for Surface Wind Prediction around Qatar. *Journal of Atmos. And Ocean. Techn.* 35, 575-592. <https://doi.org/10.1175/JTECH-D-17-0125.1>
- Senafi, F.A., Anis, A., 2015. Shamals and climate variability in the Northern Arabian/Persian Gulf from 1973 to 2012. *Int. J. Climatol.* 35, 4509-4528. <https://doi.org/10.1002/joc.4302>.
- Shanas, P.R., Aboobacker, V.M., Albarakati, A.M.A., Khalid, M.Z., 2017. Climate driven variability of wind-waves in the Red Sea. *Ocean Modelling* 119, 105-117. <https://doi.org/10.1016/j.ocemod.2017.10.001>.
- Sirisha, P., Sandhya, K.G., Balakrishnan Nair, T.B., Venkateswara Rao, B., 2017. Evaluation of wave forecast in the north Indian Ocean during extreme conditions and winter monsoon. *J. Operational Ocean.* 10, 79-92. <https://doi.org/10.1080/1755876X.2016.1276424>.
- Thoppil, P.G., Hogan, P.J., 2010. Persian Gulf responsetoa winter timeshamalwindevent. *Deep-Sea Research Part I*, 57, 946–955. <https://doi.org/10.1016/j.dsr.2010.03.002>.
- Van Dyke, J.M., 2008. *Transit Passage Through International Straits*. University of Hawaii: 216. <https://doi:10.1163/ej.9789004172678.i-786.50>.
- Vieira, F., Cavalcante, G., Campos, E., 2020. Analysis of wave climate and trends in a semi-enclosed basin (Persian Gulf) using a validated SWAN model. *Ocean Engineering* 196, 106821. <https://doi.org/10.1016/j.oceaneng.2019.106821>.
- Villiers, M., Heerden, J., 2011. Nashi dust storm over the UnitedArab Emirates. *Weather* 66, 79-81. <https://doi.org/10.1002/wea.727>.
- Yu, Y., Notaro, M., Kalashnikova, O.V., Garay, M.J., 2016. Climatology of summer Shamal wind in the Middle East. *J. Geophys. Res. Atmos.* 121, 289–305. <https://doi.org/10.1002/2015JD024063>.